Motor primitives are determined in early development and are then robustly conserved into adulthood

Qi Yang[a], David Logan[b], and Simon F. Giszter[b,c,1]

[a]Department of Neurology & Orthopedics, Columbia University Medical Center, New York, NY 10032; [b]Neurobiology and Anatomy, Drexel University College of Medicine, Philadelphia, PA 19129; and [c]School of Biomedical Engineering, Science and Health Systems, Drexel University, Philadelphia, PA 19129

Edited by Emilio Bizzi, Massachusetts Institute of Technology, Cambridge, MA, and approved May 2, 2019 (received for review December 20, 2018)

Motor patterns in legged vertebrates show modularity in both young and adult animals, comprising motor synergies or primitives. Are such spinal modules observed in young mammals conserved into adulthood or altered? Conceivably, early circuit modules alter radically through experience and descending pathways' activity. We analyze lumbar motor patterns of intact adult rats and the same rats after spinal transection and compare these with adult rats spinal transected 5 days postnatally, before most motor experience, using only rats that never developed hind limb weight bearing. We use independent component analysis (ICA) to extract synergies from electromyography (EMG). ICA information-based methods identify both weakly active and strongly active synergies. We compare all spatial synergies and their activation/drive strengths as proxies of spinal modules and their underlying circuits. Remarkably, we find that spatial primitives/synergies of adult injured and neonatal injured rats differed insignificantly, despite different developmental histories. However, intact rats possess some synergies that differ significantly, although modestly, in spatial structure. Rats injured as adults were more similar in modularity to rats that had neonatal spinal transection than to themselves before injury. We surmise that spinal circuit modules for spatial synergy patterns may be determined early, before postnatal day 5 (P5), and remain largely unaltered by subsequent development or weight-bearing experience. An alternative explanation but equally important is that, after complete spinal transection, both neonatal and mature adult spinal cords rapidly converge to common synergy sets. This fundamental or convergent synergy circuitry, fully determined by P5, is revealed after spinal cord transection.

motor primitives | muscle synergies | pattern generation | spinal cord injury | development

Motor patterns can show significant modularity in legged vertebrates. Modularity can take several forms (1). Here, we examine modular motor drives in spinal systems. This approach combines both structural and functional neural components. The fundamental idea is that basic movement is largely composed of small numbers of synergies or motor primitives, which act as building blocks (1–5). Synergies for this study are defined as spatial synergies (1), which each represent a premotor drive to motor pools, causing covarying muscle activity in a specific balance. Such drives could arise from a well-defined neural substrate of sets of neurons with specific premotor connectivity. Indeed, some data in frogs and monkeys support this idea (6, 7). Such modularity could arise as follows: first, directly through evolutionarily determined processes in development; second, through plastic online optimizations during development; third, de novo during motor skill learning; or fourth, via some combinations of these (1, 2, 4, 8). The collection of synergies resulting from any of these processes can form a library of compositional elements useful both for new movement construction and for the standard repertoire of the individual. If optimization/learning organizes the modularity of adult synergies, then modules might be unique to individuals, reflecting life experiences. Such synergies and circuits could be altered significantly in adults compared with young animals. Alternatively, if evolution and development determined a modularity matched to anatomy and common default tasks (breathing, locomotion, feeding, or grooming), then modules in all individuals of a species could be similarly structured. All would possess similar and robust motor primitives/synergies. Which option occurs has been unclear. Furthermore, it has been unclear if modularity and pattern that are observed in the spinal cord in early life are preserved and remain available later in the intact or injured adult nervous system (1, 4, 5). One confound is that, just as motor experiences may shape synergies similarly through either ontogeny or adult optimization, so too natural selection-based evolution would shape fixed modular circuits on longer timescales. These timescales and factors can be disentangled only by comparing animals with strongly differing developmental motor histories. To achieve this, we leveraged spinal cord injury (SCI) to discover if common synergy structures arise after both early postnatal and adult spinal transections.

Response to SCI in mammals differs from that in lower vertebrates, which show significantly greater regenerative capacities. This regenerative difference might originate in the higher flexibility and complexity of development in mammals. However, responses to injury between young and adult mammals are also very different. Some (~20%) rats (9–17) and also, very young kittens (18) with complete spinal transections can show remarkable levels of function as adults compared with equivalent adults with similar injuries sustained as adults. Specifically, if injuries occur before postnatal day 5 (P5), some rats and cats can walk over ground with autonomous balance and weight support using all four limbs as adults. They attain a remarkable level of compensation and function given the degree of neural deficit. Furthermore, this is attained spontaneously without special rehabilitation or manipulation. Such spinalized neonatal SCI animals are the only examples known in placental mammals of spontaneous and successful

Significance

We show that major differences in postnatal experience and development do not impact the fundamental deep structure of motor primitives generated in the spinal cords of mammals. We show that the availability of core synergy structures/primitives persists into adulthood. These synergy structures in lumbar spinal cord are revealed to be closely similar among all individuals despite different motor experiences and capabilities [postnatal day 5 (P5) vs. adult transections] after a complete spinal cord transection. This similarity of synergy set after spinal transection could arise, because the synergy circuitry is fully determined at P5, because the circuitry development is equifinal despite the P5 isolation from brain, or because the circuitry plasticity converges on the same synergies after each transection.

Author contributions: S.F.G. designed research; Q.Y. and S.F.G. performed research; Q.Y., D.L., and S.F.G. analyzed data; and Q.Y. and S.F.G. wrote the paper.

The authors declare no conflict of interest.

This article is a PNAS Direct Submission.

[1]To whom correspondence may be addressed. Email: sgiszter@drexelmed.edu.

This article contains supporting information online at www.pnas.org/lookup/suppl/doi:10.1073/pnas.1821455116/-/DCSupplemental.

Published online May 28, 2019.

autonomous four-legged balance and hind limb weight support recovery in locomotion over ground, and this is achieved without special training or treatment after complete SCI. This is partly possible, because many neonatal SCI animals remain capable of generating autonomous lumbar stepping movements. The highest functioning 20% of rats are able to integrate this stepping into balanced quadrupedal and independent weight support over ground when tested as adults (10, 12–15, 17). In contrast, animals injured as adults have much more limited recovery after complete SCI (14, 19). Specifically, they do not step spontaneously. They never achieve balanced autonomous quadrupedal weight-supported locomotion over ground, although if stimulated by various means (11, 16, 18, 20–22), they can show hind limb stepping alternations, and the hind legs can then be taught to bear load during stimulation and with significant external aid for balance support. Two obvious differences between the neonatal SCI and adult SCI animals that might account for the recovery differences are (*i*) the altered developmental processes of the spinal neural networks and (*ii*) the differing potential for neural plasticity at injury. In intact adult rats, the spinal circuits underwent continuous supraspinal input and control during development and into adult life. Removal of these is catastrophic. On the other hand, after neonatal SCI, the spinal cord develops in complete isolation from the inputs of descending systems. Neonatal SCI animals' nervous systems also undoubtedly have greater plasticity. We used these differences to discover if the synergy structures in motor patterns differed fundamentally between three groups of rats: (*i*) intact adult rats and two groups of adult rats with spinal cords that were either (*ii*) fully transected and isolated from the brain early in development (P5) before any descending pathways influence or control is experienced or (*iii*) isolated in adulthood, well after development is completed.

We analyzed motor patterns of the rats as sets of muscle synergies (2–4, 23–27). A muscle synergy is defined here as a functional unit of premotor drive (1, 23–25). Spinal neural networks generate temporally varying drives, each with specific spatial distributions to different muscles [i.e., specific synergies (4, 23, 25, 28)]. The experimental and computational issue is to identify these drives. We chose independent component analysis (ICA) to identify drives and the synergy spatial distributions to muscles (23, 29). We compared synergies in intact rats ("INTACT"), the same rats shortly after complete spinal transection as adults ("ATX"), and adult rats that had received complete spinal transection as neonates ("NTX"). Rats were tested at similar ages after completion of growth to fully mature adults of ~250 g. Furthermore, to ensure that motor experiences also differed between groups, we specifically selected only the nonweight-supporting NTX rats for the NTX group. This selection meant that the motor experience of the groups of rats was as different as possible, with no significant leg loading or weight bearing ever experienced in the NTX rats used. This minimized the chance of convergent optimization processes driven by similar biomechanical experiences during development or adulthood. We hypothesized that, if synergy modules were organized in early development and were preserved into adulthood, synergies would be similar between the groups of adult rats even after very different subsequent development and biomechanical loading and motor experience. We envisioned two possible experiment outcomes. First, significant differences in modularity and synergy expression might occur between rats injured as neonates and rats injured as adults. Second, the two injured groups might be similar in synergy expression. The latter result would strongly support robust synergy structures laid out in early spinal cord development and preserved despite experience and learning. Our data below support this second alternative and the hypothesis of early organized and robustly similar synergy circuits preserved into adulthood.

Our data will show that the circuitry to support fundamentally similar modular synergies must be present and largely similar in both ATX and NTX rats and that this circuitry is likely engaged in locomotion even in INTACT rats, albeit with some modifications. Development does not fundamentally change this spinal infrastructure for synergies or motor primitives or their use in motor pattern formation by central pattern generators.

Results

In total, 21 adult female Sprague–Dawley rats received electromyography (EMG) electrode implantations in nine hind limb muscles (*Materials and Methods* and *SI Appendix*). We recorded EMG signals while intact rats walked on a treadmill at the speed of ~1 step cycle per second and while other rats attempted the same (Fig. 1). Three groups were examined. (*i*) Unoperated control rats ($n = 12$; INTACT group). (*ii*) Nine of the INTACT rats were spinalized after initial data collection and then, tested as adult transected rats ($n = 9$; ATX group) between 10 and 14 d

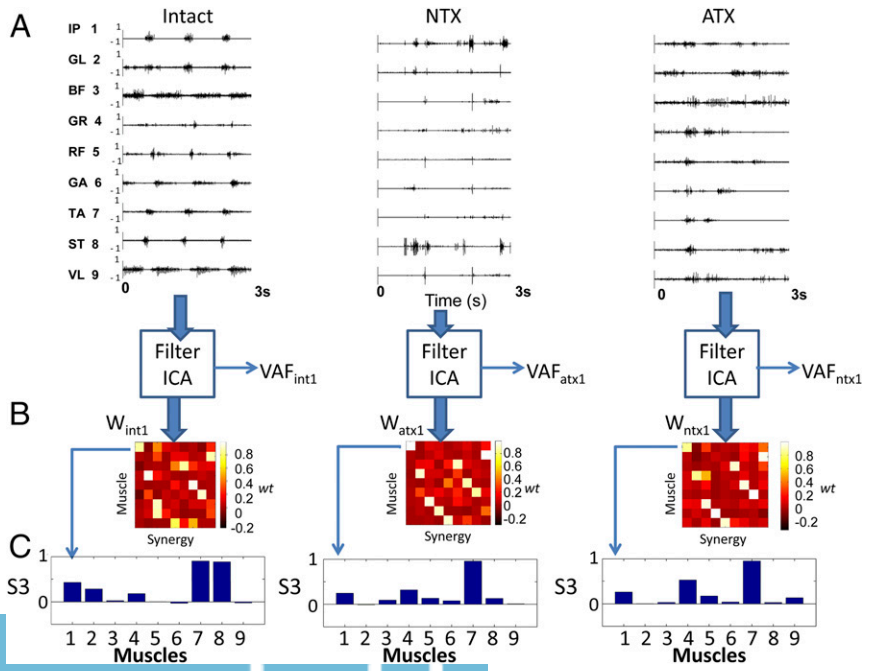

Fig. 1. Data collection and analysis. (*A*) Examples of raw EMG data from individual animals in the INTACT, NTX neonatal injured animal (animal 15), and ATX adult injured animal groups. The *y* axis is normalized voltage, and the *x* axis is time in seconds. *Left* shows the trace label (muscle recorded and its number). Nine muscles were recorded, and contributed weights in synergies were measured: 1, IP; 2, GL; 3, BF; 4, GR; 5, RF; 6, GA; 7, TA; 8, ST; and 9, VL. (*B*) Data processing procedure. EMG is rectified and rms filtered (*Materials and Methods*). ICA applied to the filtered EMG then produces a set of synergy weights (W) in a matrix (here, displayed as a heat map) and activations (not shown). The activations and W allow calculation of a cumulative VAF for all of the synergies of individual animals. There are as many synergies from ICA as muscles recorded, allowing examination of both strongly and weakly expressed synergies. (*C*) Example of one synergy (synergy 3) taken from individuals in each type of animal. Abscissa, muscle number; ordinate, muscle weight.

after the surgery as soon as testing was possible. Group mean weights were roughly similar: INTACT, 294.53 ± 8.80 g; NTX, 288.88 ± 10.39 g; ATX, 283.00 ± 9.81 g. ATX rats showed no significant motor pattern expression in hind limbs without stimulation, and therefore, tail pinches were used to elicit locomotor-like rhythmic alternation and other patterns in the ATX group. (*iii*) Adult animals that had been spinalized as neonates (day 5 or 6 after birth; $n = 9$; NTX group). NTX rats showed spontaneous alternation without tail pinch and were implanted with EMG electrodes as adults. However, by experimental design, none of the NTX rats used here were weight supporting (17). NTX, like ATX, rats walked with forelimbs, pulling the hind limbs. We collected 240 s of continuous motor activity data (only roughly resembling normal locomotion in the case of the spinal transected rats) for each animal. Sample raw recordings are shown in Fig. 1*A*. Using Bell–Sejnowski Infomax ICA (a blind separation of sources method) (29) for the EMG data, we estimated the distinct synergies underlying the elicited motor patterns. The synergy extraction method used is more effective with variable motor output and pattern rather than high stereotypy as sought in locomotor training (23). This allowed for analysis of early and less organized patterns collected shortly after SCI. For nine muscles, the ICA method estimated nine synergies (Fig. 1*B*, synergies are expressed as 9 × 9 matrices). The method separates electromyograms into source components (here, the synergies of interest) using Shannon information (i.e., by minimizing mutual information and thus, higher-order correlations among sources) rather than variance for picking synergies. This information-based technique advantage is that, if the strength of expression of a synergy changes and weakens, it will still be identified and its spatial structure will be estimated using ICA provided that the signal remained present. Variance-based methods for examination of synergy modularity and ICA outcomes are usually similar. There is almost identical dimensionality reduction of the motor pattern into a few high-variance carrying synergies (26, 28, 30–32). However, synergies can be identified in ICA even if they are only weakly expressed (i.e., low variance), and there is no assumption of the number of synergies; therefore, it is possible to discover commonalities and differences in synergies beyond the dominant high-variance dimensionality reduction into a few synergies. ICA may thus identify additional structures present in data. The limitation of ICA is that no more synergies can be discovered than muscles recorded. However, this is a universal issue in most blind separation of source methods if operating without prior knowledge of structures. We used ICA to examine modularity and its changes and to explore synergy correlation among the three types of rats. Fig. 1*C* shows muscles engaged in synergy 3 in the three groups of rats.

Contributions of Synergies to the Variance of EMG. We calculated the cumulative "variance accounted for" (VAF) for all synergies' contributions to the EMG. We combined the spatial synergies and the temporal activations of synergies from ICA to examine reconstruction of variance, as is standard (23). Unsurprisingly, the results showed that fewer than nine synergies were needed to reconstruct most of the EMG variance (Fig. 2). There was a significant dimensionality reduction. We compared how many synergies were needed to achieve 85% of cumulative VAF among the INTACT, NTX, and ATX animals (Fig. 3).

Variance contributions in nonnormalized EMG data (Fig. 2) showed a statistically significant difference between the three groups of animals [one-way ANOVA; $F(2, 27) = 3.732$, $P = 0.037$] in the synergies needed to achieve 85% of EMG VAF. Post hoc Bonferroni-corrected tests showed that the number of synergies needed was significantly fewer in the ATX animals (2.89 ± SD 0.93) compared with INTACT animals (4.00 ± SD 0.85, $P = 0.034$) (Fig. 3). NTX neonatal spinalized animals needed on average 3.44 ± SD 1.01 synergies to achieve 85% EMG VAF. NTX synergy number did not differ significantly from those of INTACT and ATX animals. These differences were also robust to using a less stringent level of 80% of VAF

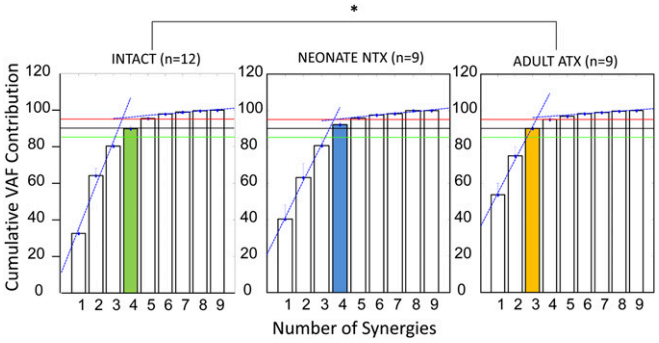

Fig. 2. The number of synergies needed cumulatively to achieve 85% of EMG variance difference between animal groups. Average cumulative VAF plots are shown for each group of rats. Abscissa is synergy number. Ordinate of the cumulative bar chart is VAF (maximum of one). These three plots differ between the three groups of animals, and each plot shows a sharp elbow. Usually, this elbow would be used to estimate the number of synergies needed to reconstruct EMG signal well and thus, the reduction in degrees of freedom due to high-variance synergies. The green horizontal line indicates 85% of EMG contribution, the black horizontal line indicates 90% of EMG contribution and the red horizontal line indicates 95% of EMG contribution. The colored bars in each graph (green in INTACT, blue in NTX, and orange in ATX) represent the average number of synergies needed to achieve at least 85% of VAF in each animal group. Error bars represent SEMs. The number of synergies needed to achieve 85% of EMG contribution differed between ATX and INTACT animal groups. The number of synergies needed in the INTACT rats differed significantly from that of the ATX rats. No significant differences were observed between INTACT and NTX or between NTX and ATX. Animal numbers used: INTACT animals, $n = 12$; neonatal SCI animals, $n = 9$; adult SCI animals, $n = 9$. *$P < 0.05$.

criterion. The variance differences are consistent with observations that central nervous system (CNS) injury causes fewer synergies to be required, with possible merging and collapse of synergies (27, 33–40). The reduced numbers of higher-variance synergies in the ATX group here, with merging or collapse of parts of the patterns as consequences, would reduce flexibility and generate motor deficits in the ATX group of rats compared with the NTX and INTACT rats.

Correlation of Synergy Weight Matrices Between Groups. We next examined whether the spatial structure of synergies (i.e., the actual muscle composition of synergies) differed among the INTACT, NTX, and ATX animals. These differences could be assessed by comparing individual synergies selected from all of the synergies expressed by two animals (e.g., selecting synergy 3 in Fig. 1*C* or Fig. 4*A*) or by comparing the synergies as ensembles as provided in the ICA-derived "synergy weight matrix" comprising all of the synergies in the animals. We first compared ensembles (Fig. 4*B* shows example matrices). Note that these analyses were independent of the VAF reconstruction analysis.

For the ensemble analysis, we initially sorted the weight matrices comprising the spatial structure of all of the synergies in each animal to align each matrix with a common template. The common template was chosen from among all of the animals in the study. As in prior work (23), we used the animal's weight matrix that had the highest correlation over all synergies to all of the other animals across all groups as the template. This was an NTX rat (synergies are shown in Fig. 4*A*). All matrices and synergies of other animals were then sorted to this template for an optimal matching. The template matrix synergy weights are shown in Fig. 4*A*. Fig. 4*B* shows nine individual rat matrix examples, three from each group, all sorted to best match the template synergy. All of the animals matrices correlated well with the common template, meaning that synergies overall were not very different among groups. Average synergy weight matrices for each group are shown in Fig. 4*C*. These were again very similar in each group. On average, the correlation value to the common template matrix was 0.92 for the INTACT group rats, 0.96 for NTX, and

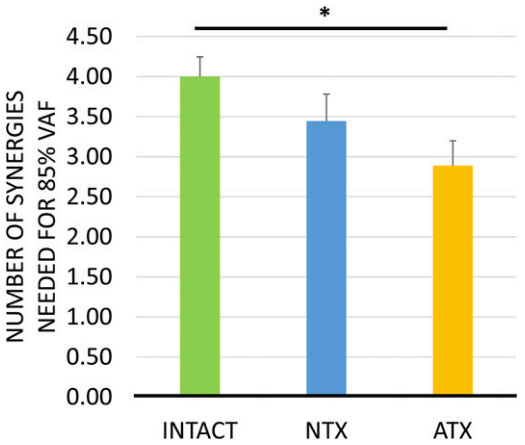

Fig. 3. Number of synergies needed to achieve 85% EMG. The figure shows the mean contribution needed in each group of rats, representing the conventional modularity of the patterns expressed. The number of synergies needed differed between the animal groups. Error bars represent SEMs. Animal numbers are the same as in Fig. 2. $*P < 0.05$.

0.95 for ATX animals (Fig. 5*A*). In effect, the synergy compositions of all of the rats tested correlated well with the template matrix and its component synergies, with overall correlations greater than 0.9.

Despite overall similarity, ANOVA analysis of correlations showed significant differences, with post hoc differences of INTACT rats from the other groups. We tested first using the raw correlations, with significant differences between INTACT and NTX and between INTACT and ATX using least significant difference (LSD) corrections. However, because correlations are usually nonnormal in distribution (and in these data, skewed to high correlation values), we repeated the analysis using the Fisher *Z* transform of correlations. This enforced normality on the data and thereby, avoided false positives. The differences in correlation to template of INTACT rats from the others remained significant with LSD correction, with Bonferroni correction for multiple comparison showing significant differences between INTACT and NTX.

INTACT rats differed significantly from the others, but ATX and NTX groups did not differ from one another. However, the ATX rats were created from the same INTACT adult rats by complete spinal transections; thus, our data suggest that a common synergy-generating circuitry is present both in INTACT rats (acting as controls with normal development) and in the NTX rats in which the spinal cord was deprived of all supraspinal pathway inputs at 5 d after birth and beyond. The common synergy infrastructure was altered in expression in the INTACT rats, but after the spinal transection experiment (in ATX rats), it appeared that the same sets of synergies as in NTX rats were revealed or that the outcome had similar plasticity. Such synergy structures present and conserved in both groups would thus be available across all individuals and ready to be engaged by rehabilitation, connected by regenerative controls, promoted through therapy, or targeted by bionic and neuroprosthetic tools.

We next examined in more detail the matrix correlations of individual rats with one another rather than just with the template matrix. For this analysis of correlations, the synergies' ordering in the matrix was not constrained to the template synergy order, but instead, synergy orders were optimized within each individual matrix pairing, by using the MATLAB tools matcorr and matperm. Thus, each correlation of matrices was the best possible correlation. This avoided the possibility that the imposed template ordering used in Fig. 5*A* was in some way the source of the statistical differences. We examined the matrix correlations of each rat with all others and plotted these for each group as clouds of points in three dimensions (Fig. 5*B*). The matrix correlation values of the INTACT group of animal's spatial synergy structure compared with all of the other animals (neonatal injured NTX and adult injured ATX animals) spanned a larger volume and greater ranges than those of the NTX and ATX rats (Fig. 5*B*). This was consistent with significant differences between the INTACT group rats and the other two groups in which correlation values tended to cluster together. This is also seen clearly in Fig. 5*C*, where two-dimensional (2D; false color) "heat" map representations of individual INTACT animal's synergy matrix correlations to either the NTX (Fig. 5*C*, *1*) or the ATX animals' synergy matrices (Fig. 5*C*, *2*) and correlation between NTX and ATX rats' synergy matrices (Fig. 5*C*, *3*)

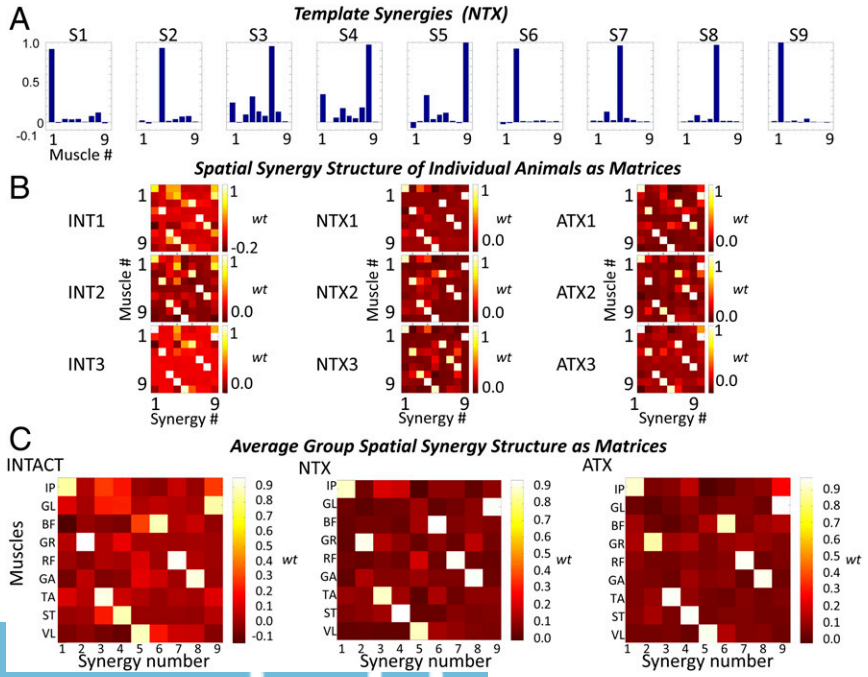

Fig. 4. Spatial structure of synergies within each animal group. (*A*) Synergies weights observed in the common NTX template animal used to order all synergies in template-based analyses. This synergy set represented the animal that was the closest in its pattern compared with all other animals. (*B*) Synergy spatial structures from three exemplar animals in each group are shown as weight matrices, with each displayed using a common color mapping for each animal in the group. The *x* axis represented synergies 1–9. The *y* axis represents individual muscle's weight in each synergy. There were nine muscles' weights in each synergy. The muscles were ordered as in Fig. 1: 1, IP; 2, GL; 3, BF; 4, GR; 5, RF; 6, GA; 7, TA; 8, ST; and 9, VL. (*C*) Average weight matrix representation of synergies' spatial structure by group displayed as heat maps. These represent averaged matrices over all animals within the animal group and thus, summarize the mean weight matrix by group. The color scales are the same for all animals, with the lighter colors representing higher weight values.

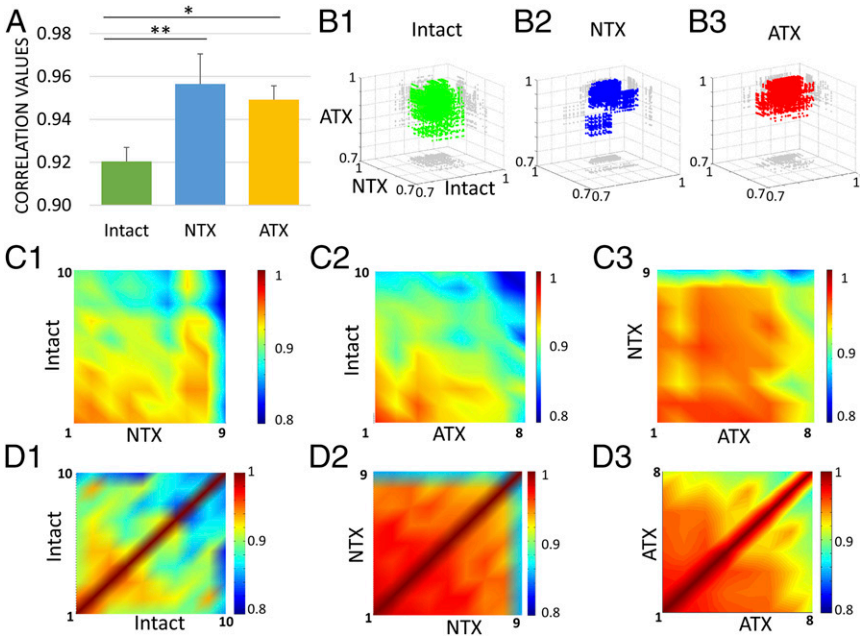

Fig. 5. Synergy weight matrix (spatial structure) correlations among and within groups. (*A*) Mean correlation to the template weight matrix for INTACT, NTX neonatal SCI, and ATX adult SCI animals. The average correlation of each animal group to the template was high in all animal groups. The mean correlation of the INTACT animals to template deviated from both the NTX and ATX animals. There was no significantly difference observed between the NTX and ATX animals. Error bars represent SEMs. $*P < 0.05$; $**P < 0.01$. (*B*, *1*) Individual INTACT animal's correlation to every other INTACT, NTX, and ATX animal as a 3D scatter plot. The gray shadows represent the projections onto the corresponding 2D plane. (*B*, *2*) Individual NTX animal's correlation to each INTACT, NTX, and ATX animal. (*B*, *3*) Individual ATX animal's correlation to each INTACT, NTX, and ATX animal. NTX and ATX rats' scatter plots are less dispersed in range compared with INTACT rats. (*C*, *1*) Correlation of each NTX animal to each INTACT animal. The correlation value is represented in the color of the matrix heat map, with warmer colors representing higher correlations. (*C*, *2*) Correlation of each ATX animal to each INTACT animal. (*C*, *3*) Correlation of each ATX animal to each NTX animal. The differences visible here are statistically significant (in the text). (*D*) Correlation of each animal to its own group in (*D*, *1*) the INTACT group, (*D*, *2*) the NTX group, and (*D*, *3*) the ATX group. Internal correlations are weakest in INTACT rats. Animals used in this figure: INTACT animals, $n = 10$; neonatal SCI animals, $n = 9$; adult SCI animals, $n = 8$ (*SI Appendix*).

are shown. INTACT rat correlations with the other two groups (Fig. 5*C*, *1* and *2*) showed colder/lower values compared with the warmer/higher correlations between neonatal injured NTX and adult injured ATX rats (Fig. 5*C*, *3*). The statistical significance of these visual differences was established by one-way ANOVA on the Fisher *Z*-transformed correlations. The analysis showed that the higher NTX–ATX correlations differed significantly from the others [$F(2, 24) = 6.693$, $P = 0.005$; Bonferroni-corrected post hoc tests: INTACT–ATX vs. NTX–ATX, $P = 0.010$ and INTACT–NTX vs. NTX–ATX, $P = 0.017$ but INTACT–NTX vs. INTACT–ATX, $P = 1.000$]. These observations are consistent with significant differences of the INTACT rats synergies from the NTX and ATX, leading to reduced correlations of INTACT matrices to both ATX and NTX rats matrices compared with those between NTX and ATX rats.

We also looked at correlation among individual rats' synergy matrices within the groups of rats and expressed these as heat maps. Again, within the INTACT group, the correlations were cooler/lower than the other within-group correlations (Fig. 5*D*). These differences were also statistically significant in the Fisher *Z*-transformed correlation data. We found that the within-group correlations (Fig. 5*D*) showed a significant group effect [one-way ANOVA; $F(2, 24) = 13.379$, $P = 0.000$; Bonferroni-corrected post hoc tests: NTX vs. INTACT, $P = 0.000$; ATX vs. INTACT, $P = 0.003$; ATX vs. NTX, $P = 1.000$]. The internal correlations in the INTACT group rats were significantly worse than correlations within both the ATX and NTX groups. INTACT rats were more individually variable in synergies. However, the within-group correlations of ATX and NTX groups did not differ.

We observed that, within the INTACT group, an animal's spatial synergy structures were less similar to the other intact animals (Fig. 5*D*, *1*) than the correlations seen within the NTX group (neonate injured to neonate injured) and within the ATX group (adult injured to adult injured) of rats. These plotted figures and statistical tests showed that, even finding the best possible correlations of matrices without any standard ordering of synergies, it remained true that synergies differed significantly between INTACT rats group and the other groups but did not differ significantly between NTX and ATX rats. Furthermore, the INTACT animals correlated less well not only with the other groups of animals but also, within group. This shows that the INTACT animals group varied more individually and therefore, may have used their synergies in more sophisticated, individual, and adjusted ways.

The spatial structure of a single synergy reflects the different muscles' weights in the synergy. Our results thus far have shown analyses of the matrices (i.e., the spatial structure of all synergies) of individual animals. When ordered according to the common template (an NTX animal) (synergies in Fig. 4*A*), these differed in INTACT rats as a group compared with NTX and ATX animals (Fig. 5*A*). In contrast, the synergy matrices in NTX and ATX did not significantly differ from each other and correlated well with the common template. These results also held for best correlations among groups. These results implied that the individual synergies of ATX and NTX rats were more similar to each other, while the INTACT synergies differed. The results also suggested that, in at least some of the synergies of INTACT group rats, the same muscles must be assigned different weights from template synergies compared with the other two groups of animals. The data implied that the individual synergies of NTX neonatal SCI and ATX adult SCI animals should be the most similar to each other, while some or all of the INTACT group animals' synergies should be different from both of these two groups. These differences would presumably arise due to alterations to some synergies or synergy replacement accomplished by the INTACT rats' descending pathway inputs, which were present and functioning ipso facto. Accordingly, we made a deeper analysis of the individual synergies' structures and the correlations of these.

Correlation of the Individual Synergies Between Groups. We next assessed individual synergies. We again used synergies ordered by their best correlation to the template matrix. This procedure provided a fixed ordering overall over the entire population of rats and in all groups tested. This consistent ordering allowed us to label synergies according to the template order, thus identifying if some groups differed in specific synergies and which of the identified synergies were most variable.

We used two analyses. We first examined the various individual synergies in the groups by comparing individual synergy correlations with the corresponding synergy in the common template (Fig. 6*A*). We thus first aligned synergies in each animal to the common template matrix. Then, we calculated the correlation value of each individual synergy to the matching synergy in the template. This was what happens automatically "behind

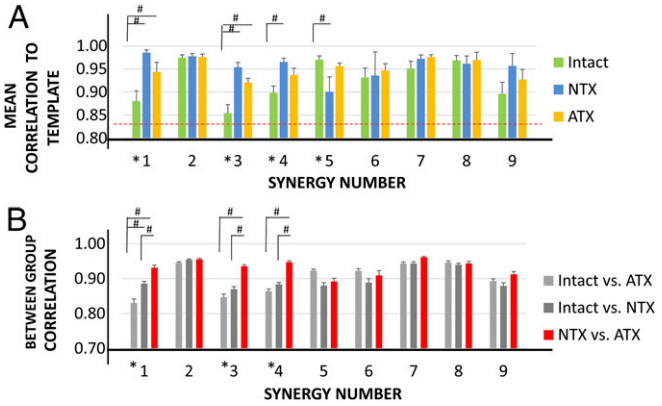

Fig. 6. Individual synergies' correlations. Synergies were sorted to template order. Animal numbers in this figure reflect some exclusions based on EMG quality (*SI Appendix*). (*A*) Correlation to template synergy. All synergies' correlations exceeded 0.85 (approximately the dotted red line). Four synergies' correlation values (synergies 1 and 3–5) showed significantly different correlations to template in INTACT rats compared with other groups. The rest of synergy correlations were similar among animal groups. No difference was observed between NTX and ATX animals in any synergy. Error bars represent SEMs. $^{\#}P < 0.05$ (significant difference in ANOVA with Bonferroni post hoc tests). (*B*) Correlation between groups of individual synergies in template order. Correlations of synergies 1, 3, and 4 were significantly higher in ATX–NTX correlations than in the matched ATX–INTACT or NTX–INTACT correlations indicated. Despite different development of ATX and NTX rats, ATX and NTX correlated better than INTACT–ATX. Animal numbers in this figure (exclusions were made of animals based on EMG quality): for synergy 1: INTACT, $n = 12$; NTX, $n = 9$; ATX, $n = 8$; for synergies 2, 4, 5, and 7: INTACT, $n = 12$; NTX, $n = 9$; ATX, $n = 9$; for synergy 3: INTACT, $n = 10$; NTX, $n = 9$; ATX, $n = 9$; for synergies 6, 8, and 9: INTACT, $n = 11$; NTX, $n = 9$; ATX, $n = 9$. $^{\#}P < 0.05$.

the scenes" in the whole-matrix correlation method. (Individual synergy's correlation values were then combined to give a single scalar correlation for the whole matrices.) Here, we examined the underlying individual synergy correlations and their differences.

All of the individual synergies in each animal correlated well with synergies in the template, as had been seen in the whole-matrix correlations. On average, the individual synergy correlation values exceeded 0.85 in all of the synergies of all three animal groups. However, the matrix differences reported between INTACT group and injured rats groups in the preceding sections reflected significant differences in specific synergies.

We again used Fisher *Z*-transformed correlations. ANOVAs showed that the correlations of synergies 1, 3, 4, 5, and 6 to template had significant group differences (*SI Appendix*, Table S1*A*). For synergies 1, 3, 4, and 5, there were specific significant differences between groups revealed in Bonferroni-corrected post hoc tests. These tests showed that correlations to the template for synergies 1, 3, and 4 of INTACT group rats were significantly lower than the NTX correlations and often, than the ATX correlations (*SI Appendix*, Table S1*C*). In contrast, in these synergies, the ATX and NTX correlations to template were both high and did not differ from one another. Synergy 5 differed from the others in that it showed higher correlations to template in INTACT rats (0.970) compared with NTX rats (0.901). However, all correlations in synergy 5 were high and were also higher that the INTACT correlations to template in synergies 1, 3, and 4. Thus, overall, NTX and ATX rats' groups showed no significant post hoc differences between them, but INTACT group rats did differ in some synergies from one or both of these groups. It is also notable that the INTACT group rats were not different from the other two groups in five of nine synergies in the post hoc tests. In three of the differing synergies, INTACT correlations to template were significantly lower than the other groups, suggesting synergy changes. In synergy 5, post hoc significance was because INTACT rat correlations were higher than NTX (both exceeded 0.9, thus deviating very little in practice). The "correlation to template" synergy analysis in Fig. 6*A* thus supported strong similarity of ATX and NTX synergies and selective changes in three synergies for the INTACT rats.

In a second analysis, we examined the direct correlations of individual synergies among all rats and between all groups after aligning them to the template. This analysis was important to further test individual synergy correlations and differences within and between groups. The analysis ensured that the NTX and ATX similarity in correlation to template reflected significantly higher correlations between the groups of matched synergies themselves tested directly. This was not guaranteed to be the case a priori. Fig. 6*B* presents plots of the mean values for individual synergies of the three pairwise correlations between the INTACT, NTX, and ATX groups. We calculated the correlation of each synergy in each animal to the corresponding synergies of each animal in the other groups (Fig. 6*B*, one-way ANOVA) or within the same group after ordering according to the template matrix. We examined within-group synergy correlations (not shown in the figures). We again used the Fisher *Z*-transformed data in all statistical tests to avoid possible type I errors. We found first that the internal correlations among rats within each group differed significantly, with within-group overall mean correlations of INTACT 0.898, NTX 0.936, and ATX 0.937. [Two way ANOVA with group and synergy as factors: $F(2, 26) = 33.763$, $P = 0.000$.] The data were consistent with decreased internal correlation and increased synergy variation within the group of INTACT group rats contrasted with greater internal correlation and internal consistency in the NTX and ATX groups of rats in which the spinal cord was isolated from the brain.

The mean overall synergy correlations between groups after template ordering were INTACT–NTX 0.902, INTACT–ATX 0.901, and ATX–NTX 0.932. In the ANOVA, only synergies 1, 3, and 4 differed significantly in their direct paired correlations, while the rest of the synergies did not (*SI Appendix*, Table S1*B*). Post hoc tests showed that, in synergies where significant differences were found, these were differences between correlations of the ATX–NTX pairing (significantly higher) compared with the other two pairings with the INTACT group rats (which were lower). Thus, correlation in pairings with INTACT rats was uniformly lower (*SI Appendix*, Table S1*D*). In summary, if correlations between groups differed significantly for a synergy, this was because the mean values of NTX to ATX correlations were significantly higher compared with the correlations of INTACT to the others. INTACT rats deviated significantly from the ATX and NTX synergy patterns.

To further test this result, we next examined for each significantly differing synergy (i.e., synergies 1, 3, and 4 indirect correlation analyses) how each individual ATX rat's synergy was correlated to the corresponding synergy observed previously when the rat was INTACT. We compared this correlation with the same rat's mean ATX synergy correlation to corresponding NTX group synergies. We tested significance using a paired one-tailed *t* test on Fisher *Z*-transformed correlations. In two of the synergies (synergies 1 and 4), the differences of correlation were significant, and in synergy 3, it was nearly significant. This analysis showed that these synergies in the group of ATX rats correlated better to the corresponding synergies of the NTX group rats than when instead correlated to themselves as individuals before spinal transection (synergy 1, $P = 0.035$; synergy 3, $P = 0.057$; synergy 4, $P = 0.020$). This strongly suggests a reversion of some INTACT synergies to an early developed and common synergy set after the ATX rats' injury and again, supports a strongly conserved core circuitry.

In summary for spatial synergy, NTX rats tested as adults were largely similar to ATX rats, with no significant changes in muscle structure and balance detectable between the NTX and ATX rats. In contrast, in INTACT group rats, three of nine synergies differed significantly, and in ATX rats, these synergies were more similar to NTX synergies than to those obtained in the same rat while intact. The synergies that differed in INTACT

group rats seemed to revert back to the NTX/ATX pattern in the spinal cord isolated from the descending pathways inputs.

Variance Contributions of the Top One to Five Synergies. Variance in our analyses can be used as a proxy for the strength of expression of a specific premotor drive in the motor pattern. The two analyses in the preceding section showed that several of the higher variance-capturing locomotor synergies that were used in NTX rats (i.e., synergies 1, 3, and 4) differed significantly in their correlation to template synergies in the INTACT group rats but not in ATX rats. We showed synergy spatial similarity in NTX and ATX rats by examining correlations and alignment to template. However, the analyses above did not consider variance captured or power of expression of these specific synergies in each of the motor patterns of INTACT, NTX, and ATX rats and whether these differed. We wanted to understand if INTACT and ATX rats used the same highly correlated synergies as strongly in their motor activity as NTX rats. We had thus far shown that synergies detected as motor drives were still available, but these could still be very weakly or very little used in different groups of rats. Significant cumulative variance changes found among the rat groups were already noted above in VAF analyses (Fig. 2). We asked whether the INTACT and ATX rat synergies that corresponded to synergies 1–5 in NTX rats (i.e., those in NTX of high variance) were also among the highest variance-capturing synergies (and thus, were expressed strongly) in the INTACT and ATX rats. Synergies might be similar in spatial structure, but their contributions greatly reduced in the two groups of normally developed adults. We found the top five synergies contributing to variance in each rat in each group. We then sorted these synergies in each rat according to the NTX template used in Figs. 5*A* and 6. We reasoned that, if those synergies with high power in NTX rats in Fig. 2 remained high power in ATX and INTACT group rats, then the probability of these synergies occurring among the top five NTX ordered would be high. In contrast, if the synergies with high power were largely random or if they differed strongly from the NTX order, then the probability would be lowered. For each synergy in the NTX top five (synergies 1–5) in each type of rat, we calculated the percentage of animals in which it was a top five synergy (Fig. 7).

Using a Fisher exact test under the null hypothesis assumption that the probability of a synergy placement in the variance order is random but that the five synergies must all be placed (i.e., we used a hypergeometric distribution), the probability of the actual distribution observed (or better) in each animal was calculated using the MATLAB function hygecdf(). We then calculated the probability of the observations in each group to determine if each group distribution was significantly nonrandom and higher or lower than expected. We expected that, in the NTX population (n = 9), the first five synergies would be clustered strongly in the higher-variance places in order (and very similar to the NTX template), and the Fisher exact probability of finding these observations under a random draw assumption was indeed P = 1.8E-8, thus reflecting this. However, it is worth noting that there were expression variations even within the NTX group. The average percentage of synergies in the high-variance category relative to the template order was 75.6% [i.e., less than perfect (100%)], perhaps reflecting variations in rhythmic recruitment of synergies among the nonweight-supporting rats. The probability of the clustering in higher-variance order that was seen in the group of INTACT rats (n = 12) having occurred by chance was P = 5.8E-6. Thus, in INTACT group rats, there were many more high-power synergies matched to NTX than could be attributed to chance. There was a persistent strong use of the synergies that NTX rats also used strongly. The average percentage of synergies in the high-variance category relative to the template 100% in the INTACT rats was 68.3%. Finally, the probability of the clustering observed in ATX rats (n = 9) was P = 1.6E-5, again much higher than could occur by chance. The average percentage of synergies in the high-variance category relative to the template 100% in the ATX rats was 60.0%. Thus, the synergies corresponding to the higher-variance synergies in the template NTX rat also, on average, remained higher-variance synergies in the other types of rats. However, we observed that there were some synergies that clearly dropped off in power and differed among groups. Fig. 7 shows two specific synergies (synergy 2 in INTACT rats and synergy 3 in ATX rats), both of which largely dropped out of the high-variance group. Interestingly, the muscle composition of synergy 2 in both INTACT rats and ATX rats remained strongly correlated to synergy 2 in NTX rats (Fig. 6), with no significant difference in correlation among groups. However, INTACT group rats used synergy 2 only weakly. In contrast, synergy 3 in INTACT group rats altered significantly in its correlation with the NTX rats' synergy 3, but this change did not happen in ATX rats as shown in Fig. 6. Nonetheless, synergy 3 was strongly reduced in its power contribution in the ATX rats, although not in the INTACT rats. These changes likely reflect differences in the rhythmic use of the synergies and in the synergy recruitment processes among the groups during pattern generation. The differences observed were likely under the influence of descending pathways in INTACT group rats and occur as a result of maturation-driven motor learning. The changes in ATX rats may represent the immediate effects of the sudden absence of such descending controls after adult spinal transection. These two specific synergies and synergy 5 are likely points of alteration in the INTACT adult motor pattern during development. These changes may represent significant differences in control of pattern formation and pattern generation in intact rats after normal maturation.

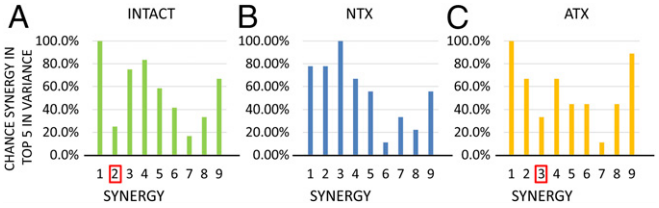

Fig. 7. The probability that similar synergies were expressed with high-variance activation among groups. Chance that an individual synergy was one of the top five contributors is plotted after matching the synergies to template order: (*A*) INTACT, (*B*) NTX, and (*C*) ATX. The chances of synergies 1–5 as a group being among one of the top five contributors after ordering according to template correlation were largely similar among the three groups of animals and were all significantly greater than chance, indicating strong use of these five in all three groups. However, two synergies from these five clearly differed (red squares in *A* and *C*). Synergy 2 had a significantly lower chance of being one of the top five contributors in the INTACT rats than in the NTX and ATX animals. Synergy 3 had a significantly lower chance in ATX rats than in INTACT or NTX rats. Although synergy 2 was not altered in INTACT rats, it was not used strongly. In contrast, synergy 3, which was altered in INTACT but not in ATX, was weakly activated in ATX, perhaps after short-term loss of some descending drive or modulation after the injury.

Discussion

Our data show that motor production in mammalian spinal cords reverts to a basic set of synergy drives or primitives after complete spinal cord transection. The basic set of synergies was in common across all individuals tested after removal of descending pathway inputs and likely largely determined shortly after birth. The set was very similar between adult spinal cords isolated from the brain as adults and rats in which the lumbar spinal cord was isolated from brain influences on P5. Furthermore, the rats here also differed in the biomechanical loads experienced and thus, the sensory reafferent experience: NTX group rats never had significant experience of any loaded hind limb weight support. Thus, both neural controls experienced and mechanical load in the legs through development were different between the groups. Despite these differences, the spinal cords expressed similar drives and primitives after adult spinal transection. In fact, the ATX rats were more similar in motor production and correlation to the NTX rats spinal transected shortly after birth than they were to themselves when previously tested in the INTACT able-bodied condition. The data here thus

suggest that either (*i*) the early infrastructure for primitives is fully preserved into adulthood in intact rats or (*ii*) the core lumbar spinal cord infrastructure for primitives develops in an equifinal way such that, after complete SCI and short-term plasticity, similar synergies will result, regardless of the prior presence or absence of descending controls or of nonmatching load experiences.

To examine synergies, we used blind separation of sources with Infomax ICA. Prior research has shown that ICA, nonnegative matrix factorization (NNMF), direct component analysis (DCA), and other methods almost invariably all converge on the same modularity and sets of drives (4, 26, 28). The higher-variance drives responsible for the major dimensionality reduction are usually the focus (26, 28, 30, 32). ICA as used here is an informational rather than variance-based method of source separation. The added value of ICA is to separate all possible drives, some of which might be only very weakly expressed in some rats but dominant or strong drives in others. Furthermore, ICA did not depend on repeatable burst structures or burst phasing as does the DCA method. It could estimate synergy weights as well as synergy membership, even in relatively poorly organized nonrhythmic motor activity. Synergies could thus be examined before any rehabilitation or well-organized locomotion. Effectively, we could compare muscle weights of synergies/primitives even in weakly expressed synergies, in ordered or disordered patterns, and between every animal in each group, even if only a few synergies accounted for the bulk of EMG variance. Indeed, the number of synergies accounting for 85% of variance differed significantly among groups, but with ICA, this did not prevent comparison of the structures of the motor drives. ICA separates as many drives as there were muscles recorded available for statistical comparisons. In summary, ICA enabled us to test for weak or relatively "covert" drives in modularity analyses and revealed what is preserved and what is altered, beyond simply the strongest synergy expressions.

Our data show equifinal development or plasticity of core synergies or else, relatively hard-wired development of these synergies at an early age. This observation matches development in many other systems where core capabilities are often created before a system's use in behavior and significant feedback availability. Spinal cord development has been a model system, allowing genetic identification and tracing of neural interneuron and motoneuron classes and the construction of spinal infrastructure (41, 42). However, clearly developmental plasticity and adult motor learning must also modify expression of the systems to match individual needs. Other studies have shown significant plastic effects in rodent cords and differences between various spinal mechanisms during normal development and cords isolated from brain early in development (20–22, 43). For this reason, it is all of the more remarkable that the motor production modules, drives, or primitives do not appear to diverge from one another (or else converge again) when revealed by cord isolation in adult animals with normal development. These results suggest that a common collection of modules is likely available after neural injury across all individuals as a potential target for therapy, neuroprosthetics, and regenerative medicine.

Although we found strong conservation of drives, we did nonetheless find variations in the intact rats. Within the INTACT rats, the lumbar motor patterns and drives not only varied compared with the two groups with spinal cord isolated from the brain but also, varied more within the INTACT group among individuals. This comports with a role of learning and experience in shaping final expression of core synergies in intact adults. Although INTACT drives varied, mean synergy correlations were nonetheless never lower than 0.8 between groups and never lower than 0.85 to the best synergy template. Drives were thus altered significantly, but not radically, in intact rats. Significant changes took two forms. First, strong and significant changes in synergy weights in intact rats were restricted to a few specific synergies. Second, some synergies were not altered in weights but instead, ceased to be used strongly in patterns. Both of these types of changes are likely significant in motor drive infrastructure, pattern generation, and the pathologies and injury effects where synergies may have impact (27, 33–40, 44–49). Synergies normally weakly activated in intact CNS that become active in disease would interfere with normal function and be pathological. Similarly, reversion of altered synergies to a developmental default synergy could limit normal pattern effectiveness. However, the core synergy patterns may also be exploited by the clinician and rehabilitation scientist in compensation and neurorecovery to support function (27). Furthermore, additional plasticity may be possible; we did not here examine synergies through chronic spinal cord isolation in the adults. Synergies explored here were identified in the first weeks after SCI and before any rehabilitation.

The two types of changes in synergy observed may represent distinct mechanisms: (*i*) modification of synergy muscle weight but not level of use in the motor patterns and (*ii*) modification of recruitment and timing in the motor patterns. The Rybak scheme of pattern generation comprises two layers: a rhythm generator above a pattern shaper, which could either contain or recruit the synergies (1); type 1 change would act on pattern shaping and synergy bases, while type 2 changes could also act on the rhythm-generating and pattern engagement mechanisms.

It is also important to consider that the data here were obtained for a quadruped. Even so, modifications of synergies were seen in intact rats. These were likely learned as the rats transitioned from crawling to parasagittal walking patterns between P14 and P21. The construction of bipedal motor behaviors in humans might conceivably cause synergies expressed in walking and running in able-bodied adults to depart still further from the early default synergies or show more pervasive individual variations and suppressions than in the rats (36–38, 50). Our work here suggests that a core set of synergies in common in all individuals may nonetheless underlie aspects of these variations (27, 37, 44, 49). However, although there are well-established and significant evolutionary parallels (4) in overall pattern generation and modularity, the details of synergy adjustments across different species remain to be better understood. We speculate and suggest based on the data here that most species likely possess a developmentally conserved set of synergies/primitives and related interneuronal infrastructure when observed within a few days after spinal cord isolation in the adult.

What is the value of conserved modular collections of synergies and their persistence in the adult CNS? One perspective from human studies is that these are a remnant of a bootstrap used for learning of early and adult behavior and simply seed and speed the subsequent acquisition of skills. However, an alternative is that these continue serving valuable functional roles. First, these may be the substrate for sculpting the adult synergies as shown in our data here: while some synergy deviations are significant, strong synergy similarity persists in the INTACT group. Second, the synergies might represent components of default reflex protective behaviors held in reserve for emergency, but evolutionarily significant, eventualities (e.g., reminiscent of built-in aquatic escape behaviors mediated by Mauthner cell) (51). Some synergies may represent near-optimal ways of exciting limb dynamics (52), often essential in reflexive escape and protective motor patterns. The synergies from this perspective will also form a useful point of departure for any novel adult motor learning in new contexts. Near optimality and coadaptation of synergy and limb dynamics could arise from the coevolution of the biomechanical structure and neural control. The anatomical limb structure and biomechanics determine a feasible force space, which can be considered an evolutionary determined estimate of needs for survival actions and force delivery [in the works of Valero-Cuevas and coworkers (53, 54)]. Similarly, high degrees of freedom in the limb and body mechanics may most often be used during the lifespan in simpler ways. This relative stereotypy of routine (and often, evolutionarily critical) actions may favor "built-in" starting points for these common motor behaviors and also, favor new learned behaviors built on these. Such built-in neurally constrained solutions to the degrees of freedom problem would be based on an evolutionary derived "estimate" of the fundamental and most repeatable "satisficing"

requirements. After seeding motor learning, these synergy circuits would form as a useful backup system or be engaged in the normal repertoire. The circuits could be further tuned or transcended by additional brain controls. More complex controls are clearly needed for an individual to fully "inhabit" and exploit their biomechanics flexibly during the adult lifespan (24–26, 55–58). Other work (27, 36) has identified consistent synergies after adult SCI and similarity of these to adult intact patterns, but the developmental origins of these and how much descending control of early synergy patterns alters or reorganizes these have never been clear. To us, persistent core circuitry that is constructed early in development and then, robust throughout life is the most parsimonious explanation of the data here.

Until this study, the persistence of an early determined core infrastructure for motor synergies and primitives persisting into adulthood in mammals was an open question. Our data support such a common core synergy collection in spinal cord, which is available across individuals and across development either through equifinal plastic or through hardwired mechanisms. This infrastructure seems to be determined or laid down early in development and remains robust, persisting unaltered across very different developmental trajectories. The interneuronal and genetic underpinnings of this infrastructure and its robust persistence through differing developmental and learning processes must next be better understood and elaborated (41, 42). Similarly, we need to determine how these synergies are engaged in or altered by rehabilitation frameworks and other therapies to translate these data to better outcomes after disease and trauma.

Materials and Methods

General Procedures. We compared muscle synergies in 12 intact adult Sprague–Dawley rats, 9 adult rats spinalized at spinal segment T9/10 as neonates (~P5–P6), and 9 adult complete SCI rats derived from the 12 intact rats. All procedures were in accordance with US Department of Agriculture and Institutional Animal Care and Use Committee (IACUC) guidelines and had Drexel IACUC approval. For intact and neonatal SCI animals, EMG electrodes and a pelvis orthosis were implanted to attach a robot for subsequent rehabilitation and locomotor testing (59). Spinal transection followed after 2–4 wk in intact rats. Full technical details are given in *SI Appendix*.

Neonatal SCI Spinalization Surgery. Rats were spinalized at P5 as described in refs. 15 and 17 and detailed fully in *SI Appendix*. Transection was made at approximately segment T9/10 by aspiration of about a segment of cord, and the cavity was filled with gel foam, which prevented any potential regeneration.

Adult Spinalization Surgery. Adults rats were transected as described in ref. 14 and detailed fully in *SI Appendix*. Transection was made at approximately segment T9/10 by aspiration of about a segment, and the cavity was filled with gel foam.

EMG Electrodes Implantation. Nine muscles of one hind limb were implanted: gastrocnemius (GA), tibialis anterior (TA), semitendinosus (ST), vastus lateralis (VL), illiopsoas (IP), gluteus (GL), biceps femoris (BF), gracilis (GR), and rectus femoris (RF). These represented samples of both uni- and biarticular flexors and extensor muscles acting at three joints in the hind leg.

EMG Data Collection. For each animal, at least 240 s of EMG data were recorded. During the recording, the intact animals walked on the treadmill at the speed of 1 step cycle per second. Thus, usually more than 200 step cycles were often recorded in intact adults. After spinalization, EMG was recorded again ~10–14 d after the spinal transection injury. In adult spinalization, tail pinching was used to elicit activity.

Muscle Synergy Identification and Analysis. The collected EMG signal was first rectified. The 2-kHz data were filtered using a 40-point moving average rms filter followed by down-sampling to 250 Hz. For synergy analysis of EMG, ICA was used (23, 29) (the Makeig Matlab implementation of the Bell–Sejnowski algorithm in EEGLab). This assumed that the collected EMG signals were a linear mixture of unknown sources originating from the spinal neural networks, and these sources were independent from each other. The algorithm separated sources by minimizing the mutual information and maximizing the statistical independence of the putative source signals.

ICA generated the same number of sources as inputs. ICA did not identify any variance-based dimensionality reduction present and instead, separated as many sources as there were EMG signals on an informational basis. Nine muscles were recorded; thus, nine synergies were generated by ICA. In frogs, such analyses applied to unfiltered EMG data showed that one synergy equaled one muscle, because the highest-frequency information was independent in the EMGs (23). Thus, ICA was not "doomed to succeed" in aggregating muscles or variance. We used nonnormalized EMG in variance analyses. We hypothesized that fewer than nine synergies were needed to account for criterion variance in most behavior activities (4, 23, 27). The number was determined from the cumulative VAF. VAF curves found here had sharp elbows.

The analysis results from the ICA were the temporal and spatial structures of the synergy. The spatial structure showed individual synergy's composition of muscles and each muscle's weight in a particular synergy. The temporal structure described the activation patterns of synergies. In the case that fewer than nine muscles' EMGs were recorded in a recording session, the temporal and spatial structures for the missing muscles were set to zero, and these data were excluded from individual correlation comparison analysis (see below).

Synergies Contribution to the EMG. ICA provided synergies as a spatial structure—mixing matrix "W"—and a temporal structure—activations "C." Combining the temporal and spatial structures, we were able to reconstruct the EMG signals to some level of fidelity by using only some or all of the extracted synergies. For subsets of synergies, we calculated the percentage VAF for these synergies in EMG reconstruction, reflecting their contribution to the total EMG data. The numbers of synergies needed to achieve a criterion VAF were compared between groups.

Comparison of Synergies. To perform the comparison of muscle composition and weights in synergies across groups, the synergies of individual animals were sorted so that similar synergies were held in a similar order among all animals. To minimize the resorting process, all of the animals' synergies were sorted based on a common template. The template matrix was chosen from among all of the animals (intact, neonatal SCI ,and adult SCI animals) using an inner product column similarity measure. The animal with synergy spatial structure that had the highest overall correlation to all of the other animals was chosen as this common sorting template as in ref. 23: here, an NTX rat. Synergy weights could range from −1 to +1 in the weight matrix in principle. In practice, mostly all weights were positive between zero and one. Synergy weights were correlated in MATLAB and SPSS to obtain a Pearson correlation for the synergy. Matrices were correlated using MATLAB matcorr() and matperm() to find the best correlation possible (free order) and matcorr() when working with a fixed (template) order. For statistical comparison, correlation distributions were subject to the Fisher Z transform. Correlation statistics were tested using ANOVA and Bonferroni-corrected post hoc tests using SPSS. To avoid false precision and sample numbers, mean correlations among individual rats were calculated, and the rat number in group was used in all statistical tests.

Histology. Nissl myelin staining was used to confirm the completeness of the SCI in postmortem histology after animals finished the training process (13–15, 17). All of the animals in this study showed absence of Nissl body and myelin at the transection site (i.e., each animal used in this study showed a histologically complete SCI).

ACKNOWLEDGMENTS. This work is supported by NIH National Institute of Neurological Disorders and Stroke Grants NS054894, NS072651, NS104194; the Craig H. Neilsen Foundation Grant 224296; and a Brody Family Medical Trust Fund fellowship. Members of the laboratory of S.F.G. assisted in animal care and data discussions. H. Kebede provided histology support, working with the Marion Murray Spinal Cord Research Center. Drs. Emilio Bizzi and Marion Murray reviewed and commented on this paper in draft.

1. S. F. Giszter, Motor primitives–New data and future questions. *Curr. Opin. Neurobiol.* **33**, 156–165 (2015).
2. E. Bizzi, F. A. Mussa-Ivaldi, S. Giszter, Computations underlying the execution of movement: A biological perspective. *Science* **253**, 287–291 (1991).
3. A. d'Avella, E. Bizzi, Shared and specific muscle synergies in natural motor behaviors. *Proc. Natl. Acad. Sci. U.S.A.* **102**, 3076–3081 (2005).
4. N. Dominici *et al*., Locomotor primitives in newborn babies and their development. *Science* **334**, 997–999 (2011).
5. M. C. Tresch, A. Jarc, The case for and against muscle synergies. *Curr. Opin. Neurobiol.* **19**, 601–607 (2009).
6. C. B. Hart, S. F. Giszter, A neural basis for motor primitives in the spinal cord. *J. Neurosci.* **30**, 1322–1336 (2010).

7. T. Takei, J. Confais, S. Tomatsu, T. Oya, K. Seki, Neural basis for hand muscle synergies in the primate spinal cord. *Proc. Natl. Acad. Sci. U.S.A.* **114**, 8643–8648 (2017).
8. J. N. Ingram, M. Sadeghi, J. R. Flanagan, D. M. Wolpert, An error-tuned model for sensorimotor learning. *PLoS Comput. Biol.* **13**, e1005883 (2017).
9. D. J. Stelzner, W. B. Ershler, E. D. Weber, Effects of spinal transection in neonatal and weanling rats: Survival of function. *Exp. Neurol.* **46**, 156–177 (1975).
10. S. F. Giszter, M. R. Davies, V. Graziani, Motor strategies used by rats spinalized at birth to maintain stance in response to imposed perturbations. *J. Neurophysiol.* **97**, 2663–2675 (2007).
11. S. F. Giszter, C. B. Hart, Motor primitives and synergies in the spinal cord and after injury–The current state of play. *Ann. N. Y. Acad. Sci.* **1279**, 114–126 (2013).
12. S. F. Giszter, G. Hockensmith, A. Ramakrishnan, U. I. Udoekwere, How spinalized rats can walk: Biomechanics, cortex, and hindlimb muscle scaling–implications for rehabilitation. *Ann. N. Y. Acad. Sci.* **1198**, 279–293 (2010).
13. S. F. Giszter, W. J. Kargo, M. Davies, M. Shibayama, Fetal transplants rescue axial muscle representations in M1 cortex of neonatally transected rats that develop weight support. *J. Neurophysiol.* **80**, 3021–3030 (1998).
14. C. S. Oza, S. F. Giszter, Plasticity and alterations of trunk motor cortex following spinal cord injury and non-stepping robot and treadmill training. *Exp. Neurol.* **256**, 57–69 (2014).
15. C. S. Oza, S. F. Giszter, Trunk robot rehabilitation training with active stepping reorganizes and enriches trunk motor cortex representations in spinal transected rats. *J. Neurosci.* **35**, 7174–7189 (2015).
16. U. I. Udoekwere, A. Ramakrishnan, L. Mbi, S. F. Giszter, Robot application of elastic fields to the pelvis of the spinal transected rat: A tool for detailed assessment and rehabilitation. *Conf. Proc. IEEE Eng. Med. Biol. Soc.* **1**, 3684–3687 (2006).
17. U. I. Udoekwere, C. S. Oza, S. F. Giszter, Teaching adult rats spinalized as neonates to walk using trunk robotic rehabilitation: Elements of success, failure, and dependence. *J. Neurosci.* **36**, 8341–8355 (2016).
18. D. R. Howland, B. S. Bregman, A. Tessler, M. E. Goldberger, Development of locomotor behavior in the spinal kitten. *Exp. Neurol.* **135**, 108–122 (1995).
19. F. H. Hsieh, S. F. Giszter, Robot-driven spinal epidural stimulation compared with conventional stimulation in adult spinalized rats. *Conf. Proc. IEEE Eng. Med. Biol. Soc.* **2011**, 5807–5810 (2011).
20. P. K. Shah *et al*., Variability in step training enhances locomotor recovery after a spinal cord injury. *Eur. J. Neurosci.* **36**, 2054–2062 (2012).
21. W. K. Timoszyk *et al*., Hindlimb loading determines stepping quantity and quality following spinal cord transection. *Brain Res.* **1050**, 180–189 (2005).
22. W. K. Timoszyk *et al*., The rat lumbosacral spinal cord adapts to robotic loading applied during stance. *J. Neurophysiol.* **88**, 3108–3117 (2002).
23. C. B. Hart, S. F. Giszter, Modular premotor drives and unit bursts as primitives for frog motor behaviors. *J. Neurosci.* **24**, 5269–5282 (2004).
24. W. J. Kargo, S. F. Giszter, Rapid correction of aimed movements by summation of force-field primitives. *J. Neurosci.* **20**, 409–426 (2000).
25. W. J. Kargo, S. F. Giszter, Individual premotor drive pulses, not time-varying synergies, are the units of adjustment for limb trajectories constructed in spinal cord. *J. Neurosci.* **28**, 2409–2425 (2008).
26. N. Krouchev, J. F. Kalaska, T. Drew, Sequential activation of muscle synergies during locomotion in the intact cat as revealed by cluster analysis and direct decomposition. *J. Neurophysiol.* **96**, 1991–2010 (2006).
27. S. A. Safavynia, G. Torres-Oviedo, L. H. Ting, Muscle synergies: Implications for clinical evaluation and rehabilitation of movement. *Top. Spinal Cord Inj. Rehabil.* **17**, 16–24 (2011).
28. G. Cappellini, Y. P. Ivanenko, R. E. Poppele, F. Lacquaniti, Motor patterns in human walking and running. *J. Neurophysiol.* **95**, 3426–3437 (2006).
29. A. J. Bell, T. J. Sejnowski, An information-maximization approach to blind separation and blind deconvolution. *Neural Comput.* **7**, 1129–1159 (1995).
30. K. M. Steele, M. C. Tresch, E. J. Perreault, The number and choice of muscles impact the results of muscle synergy analyses. *Front. Comput. Neurosci.* **7**, 105 (2013).
31. K. M. Steele, M. C. Tresch, E. J. Perreault, Consequences of biomechanically constrained tasks in the design and interpretation of synergy analyses. *J. Neurophysiol.* **113**, 2102–2113 (2015).
32. M. C. Tresch, V. C. K. Cheung, A. d'Avella, Matrix factorization algorithms for the identification of muscle synergies: Evaluation on simulated and experimental data sets. *J. Neurophysiol.* **95**, 2199–2212 (2006).
33. F. O. Barroso *et al*., Combining muscle synergies and biomechanical analysis to assess gait in stroke patients. *J. Biomech.* **63**, 98–103 (2017).
34. V. C. K. Cheung *et al*., Muscle synergy patterns as physiological markers of motor cortical damage. *Proc. Natl. Acad. Sci. U.S.A.* **109**, 14652–14656 (2012).
35. D. J. Clark, L. H. Ting, F. E. Zajac, R. R. Neptune, S. A. Kautz, Merging of healthy motor modules predicts reduced locomotor performance and muscle coordination complexity post-stroke. *J. Neurophysiol.* **103**, 844–857 (2010).
36. E. J. Fox *et al*., Ongoing walking recovery 2 years after locomotor training in a child with severe incomplete spinal cord injury. *Phys. Ther.* **90**, 793–802 (2010).
37. E. J. Fox *et al*., Modular control of varied locomotor tasks in children with incomplete spinal cord injuries. *J. Neurophysiol.* **110**, 1415–1425 (2013).
38. Y. Hashiguchi *et al*., Number of synergies is dependent on spasticity and gait kinetics in children with cerebral palsy. *Pediatr. Phys. Ther.* **30**, 34–38 (2018).
39. A. Scano, A. Chiavenna, M. Malosio, L. Molinari Tosatti, F. Molteni, Muscle synergies-based characterization and clustering of poststroke patients in reaching movements. *Front. Bioeng. Biotechnol.* **5**, 62 (2017).
40. K. M. Steele, A. Rozumalski, M. H. Schwartz, Muscle synergies and complexity of neuromuscular control during gait in cerebral palsy. *Dev. Med. Child Neurol.* **57**, 1176–1182 (2015).
41. M. Hayashi *et al*., Graded arrays of spinal and supraspinal V2a interneuron subtypes underlie forelimb and hindlimb motor control. *Neuron* **97**, 869–884.e5 (2018).
42. A. J. Levine *et al*., Identification of a cellular node for motor control pathways. *Nat. Neurosci.* **17**, 586–593 (2014).
43. J. C. Petruska *et al*., Changes in motoneuron properties and synaptic inputs related to step training after spinal cord transection in rats. *J. Neurosci.* **27**, 4460–4471 (2007).
44. A. Rozumalski, K. M. Steele, M. H. Schwartz, Muscle synergies are similar when typically developing children walk on a treadmill at different speeds and slopes. *J. Biomech.* **64**, 112–119 (2017).
45. R. Ranganathan, C. Krishnan, Y. Y. Dhaher, W. Z. Rymer, Learning new gait patterns: Exploratory muscle activity during motor learning is not predicted by motor modules. *J. Biomech.* **49**, 718–725 (2016).
46. T. Lencioni *et al*., Are modular activations altered in lower limb muscles of persons with multiple sclerosis during walking? Evidence from muscle synergies and biomechanical analysis. *Front. Hum. Neurosci.* **10**, 620 (2016).
47. D. A. Jacobs, J. R. Koller, K. M. Steele, D. P. Ferris, Motor modules during adaptation to walking in a powered ankle exoskeleton. *J. Neuroeng. Rehabil.* **15**, 2 (2018).
48. J. L. Allen, J. L. McKay, A. Sawers, M. E. Hackney, L. H. Ting, Increased neuromuscular consistency in gait and balance after partnered, dance-based rehabilitation in Parkinson's disease. *J. Neurophysiol.* **118**, 363–373 (2017).
49. F. Lunardini, C. Casellato, M. Bertucco, T. D. Sanger, A. Pedrocchi, Children with and without dystonia share common muscle synergies while performing writing tasks. *Ann. Biomed. Eng.* **45**, 1949–1962 (2017).
50. H. Hirai *et al*., On the origin of muscle synergies: Invariant balance in the co-activation of agonist and antagonist muscle pairs. *Front. Bioeng. Biotechnol.* **3**, 192 (2015).
51. R. C. Eaton, J. C. Hofve, J. R. Fetcho, Beating the competition: The reliability hypothesis for Mauthner axon size. *Brain Behav. Evol.* **45**, 183–194 (1995).
52. M. Berniker, A. Jarc, E. Bizzi, M. C. Tresch, Simplified and effective motor control based on muscle synergies to exploit musculoskeletal dynamics. *Proc. Natl. Acad. Sci. U.S.A.* **106**, 7601–7606 (2009).
53. J. M. Inouye, F. J. Valero-Cuevas, Muscle synergies heavily influence the neural control of arm endpoint stiffness and energy consumption. *PLoS Comput. Biol.* **12**, e1004737 (2016).
54. C. M. Laine, F. J. Valero-Cuevas, Intermuscular coherence reflects functional coordination. *J. Neurophysiol.* **118**, 1775–1783 (2017).
55. S. A. Overduin, A. d'Avella, J. Roh, J. M. Carmena, E. Bizzi, Representation of muscle synergies in the primate brain. *J. Neurosci.* **35**, 12615–12624 (2015).
56. S. A. Overduin, A. d'Avella, J. M. Carmena, E. Bizzi, Muscle synergies evoked by microstimulation are preferentially encoded during behavior. *Front. Comput. Neurosci.* **8**, 20 (2014).
57. S. A. Overduin, A. d'Avella, J. M. Carmena, E. Bizzi, Microstimulation activates a handful of muscle synergies. *Neuron* **76**, 1071–1077 (2012).
58. S. Yakovenko, N. Krouchev, T. Drew, Sequential activation of motor cortical neurons contributes to intralimb coordination during reaching in the cat by modulating muscle synergies. *J. Neurophysiol.* **105**, 388–409 (2011).
59. U. I. Udoekwere, C. S. Oza, S. F. Giszter, A pelvic implant orthosis in rodents, for spinal cord injury rehabilitation, and for brain machine interface research: Construction, surgical implantation and validation. *J. Neurosci. Methods* **222**, 199–206 (2014).